A modern approach to QENS data analysis in Mantid

Sanghamitra Mukhopadhyay, Brandon Hewer, Spencer Howells, Anders Markvardsen

A modern approach to QENS data analysis in Mantid

Sanghamitra Mukhopadhyay*, Brandon Hewer, Spencer Howells, Anders Markvardsen

ISIS Neutron and Muon Source, Rutherford Appleton Laboratory, Science and Technology Facilities Council, Didcot, Oxfordshire, OX11 0QX, UK,

---

Abstract

Data analysis of Quasi-elastic Neutron Scattering (QENS) experiments often requires multiple steps involving fitting the elastic and quasi-elastic parts of spectra with several empirical functions and analytical models. Parameters of those models can be interdependent and also dependent on the momentum transfer vector Q. Here we present a modern data analysis interface dedicated for QENS data analysis implemented within the open source software Mantid. The interface has been implemented using the state-of-the-art design pattern Model-View-Presenter (MVP). The MVP, an architectural software design pattern, facilitates automated unit tests as well as decoupling of the business logic, presentation logic and the graphical interface. Several models are implemented for analysing both elastic and quasi-elastic parts of the dynamical scattering function $S(Q, \omega)$ and intermediate scattering function $I(Q, t)$. To understand the nature of dynamics in a QENS experiments, several models are also implemented for elastic incoherent structure factor (EISF) and jump diffusions. The interface has been validated by analysing a sample of liquid water at room temperature. The nature of hydrogen bond dynam-

Email address: sanghamitra.mukhopadhyay@stfc.ac.uk (Sanghamitra Mukhopadhyay*)

ics of the hydrogen bonded organic ferroelectric $2, 4, 5 - Br_3$ imidazole, for the first time has been analysed using this newly implemented software. It is found that protons exhibit localised random motion in this material.

1. Introduction

Quasi elastic neutron spectroscopy (QENS) is used to investigate the stochastic dynamics of atoms and molecules in solid, liquid and plastic phases of materials [1–7]. Data analysis of QENS experiments often requires multiple steps involving fitting the elastic and quasi-elastic parts of spectra and their Fourier transforms with several functions and analytical models for understanding the nature of dynamical motions. [1–3] Parameters of those models can be interdependent. The momentum transfer vector Q also becomes an important parameter for those fits. With the increase of the capability of dedicated neutron scattering instruments having high flux and high resolutions, sophisticated sample environment facilities and increasing amount of data, modern QENS experiments are performed on increasingly complex chemical systems in very challenging situations. The applicability of QENS experiments thus encompasses investigations of materials important for solving global challenges, such as liquid, biological and soft matter systems relevant to medical applications [4] to energy materials [5, 6] and movements of molecules on catalytic surfaces [8]. More sophisticated models and sustainable open source software solutions are required to analyse such data both from a Graphical User Interface (GUI) and from a scripting interface, which

2

provide ease of use for newcomers or occasionally users and option for specialist to maximize effectiveness and flexibility of analysis.

To bridge the gap of the capability of existing software for QENS data analysis [9, 10], a data analysis interface dedicated for this technique has been implemented in Mantid [11, 12]. Mantid is an open source software and many of the neutron and muon facilities across the world have already agreed to adopt it as the tool for their data reduction and analysis. Due to this reason, any software solution added to Mantid will have a long lasting lifespan with opportunity of professional maintenance. Therefore, it is the best platform to implement this analysis interface for the benefit of users across facilities.

This interface provides a user friendly graphical user's interface (GUI) with options to fit both, scattering function, $S(Q, \omega)$, and intermediate scattering function, $I(Q, t)$, with several analytical models. A sequential fitting option across multiple spectrum makes it possible to do a local-global fitting with choice of constrains and correlate spectra across Q values. This multi-dimensional (MD) data analysis interface also provides options for fitting with several models of jump diffusions and analysis of elastic incoherent structure factor (EISF). Apart from that, as Mantid provides full flexibility of using python scripting, this analysis workflow is designed in such a way that implemented models and functionalities can be used in python scripting outside the provided GUI. This freedom provides the opportunity to extend the analysis further. This scripting option is perfectly compatible with modern interactive data analysis environment, such as jupyter notebook. Users also can submit their models and analysis scripts in Mantid repository for the use of the community. Thus this implementation provides a modern approach to QENS data analysis.

QENS analysis requires a number of fitting tools to understand the mechanism of dynamics. In general low energy spectrum is fitted with a number of Lorentzians and optionally one delta function convoluted with instrument resolution to investigate incoherent scattering mechanism inside the material. A Fourier transform also can be used to get the intermediate scattering function $I(Q, t)$, which is then fitted to exponentials or derivative of exponentials to find out the molecular dynamics. The dynamics are often not that straight forward and depending on the complexities of the sample. With the upgrades of instruments and sophisticated sample environments, it is now necessary to offer more flexibility to researchers to fit several fit functions for in-depth understanding of the dynamics. This is an additional motivation for implementing a QENS analysis tool in Mantid, which already includes many in-built fit functions and minimizers and ways of adding user defined fit functions.

In this article we will discuss the implementation and features of the QENS data analysis interface in Mantid along with examples. The work on this software is on-going and its scope and future outlook for designing a fully QENS multidimensional fitting GUI will also be discussed.

2. Theory

Inelastic neutron scattering measures the total dynamic structure factor $S(Q, \omega)$ of density fluctuations, where Q is the scattering vector and ω is related with the energy transfer E between the neutron and the sample by $E = \hbar\omega$. [3, 13] $S(Q, \omega)$ can be written as a weighted sum of two contributions $S_{\text{coh}}(Q, \omega)$ and $S_{\text{inc}}(Q, \omega)$, giving information on collective motions of all particles and the correlation among the position of the same nucleus at different times, respectively. Thus $S_{\text{inc}}(Q, \omega)$

4

provides the information about the motion of a single particle.

These dynamic structure factors are related to the intermediate scattering functions by the relations [1–3]:

$$S_{coh}(Q,\omega) = \frac{1}{2\pi\hbar} \int I(Q,t)e^{-i\omega t} \tag{1}$$

and

$$S_{inc}(Q,\omega) = \frac{1}{2\pi\hbar} \int I_s(Q,t)e^{-i\omega t} \tag{2}$$

where I and I_s are coherent and incoherent part of the intermediate scattering functions, respectively.

In this article we will mainly focus on the incoherent part of the structure factor $S_{inc}(Q,\omega)$ and the intermediate scattering function $I_s(Q,t)$, hereafter called as $S(Q,\omega)$ and $I(Q,t)$, respectively.

Data analysis on QENS spectrum, i.e., $S(Q,\omega)$, are divided into two parts, an analysis of the elastic region, which generally overlaps to the energy resolution of instruments, and any broadening of the spectrum beyond the elastic region. However, this separation doesn't have clear physical meaning. The integral of the spectrum within the range of instrument resolution generally depends on Q. This integral $E_l(Q) = \int_{-\Delta\omega}^{\Delta\omega} S(Q,\omega)d\omega$, where $2\Delta\omega = FWHM$ (full width at half maximum) of the instrument resolution, is an approximation to $S_0(Q,\omega = 0)$, the dynamic structure factor for elastic scattering. $E_l(Q)$ is modeled using various functions [14–16] depending on the nature of dynamics within a material. In Mantid we have implemented three such models. Through the fitting with any of these models one can calculate mean square displacements (MSD) of the particles within the materials. One such model implemented in the current QENS data analysis interface in Mantid is the Gaussian model [14]. This model is good

for isotropic motion in homogeneous materials within harmonic potential. However, it doesn't consider motion related to vibrational or rotational and generally applicable for low Q values. In this model $E_l(Q)$ is related to MSD by the relation:

$$E_l(Q) = A_G e^{-\frac{MSD \cdot Q^2}{6}}$$
(3)

where A_G is a constant. Another example is Peters's model [15], which is good for samples having motion heterogeneity, i.e., distribution of MSD among several atoms in the sample, and is applicable for higher values of Q. The mathematical expression for this model is :

$$E_l(Q) = \frac{A_P}{\left(1 + \frac{MSD \cdot Q^2}{6\beta}\right)^\beta}$$
(4)

where A_P is a constant and β is inversely related with the degree of heterogeneity in the materials. In the limit of $\beta \to \infty$, Peters's model reduces to the Gaussian model representing homogeneous environment. Another model, called Yi's model [16] in this implementation, is good for samples with single atom motion in an anharmonic potential as well as in cases where dynamical inhomogeneity arises due to distribution of MSD among several atoms in the sample. This model considers terms up to Q^4, and so applicable for large values of Q. This model is defined as:

$$E_l(Q) = A_Y e^{-\frac{MSD \cdot Q^2}{6}} \left(1 + \frac{Q^4 * \sigma}{72}\right)$$
(5)

where A_Y is a constant and σ^2 measures the variance of MSD of all particles in the sample generally giving the width of the distribution of MSDs. In the limit of $\sigma \to 0$, Yi's model reduces to the Gaussian model.

Beyond the elastic region of any spectrum several models are used to fit either

the $S(Q, \omega)$ or $I(Q, t)$ to understand the nature of dynamics. Generally, $S(Q, \omega)$ are fitted to one or two Lorentzians, and $I(Q, t)$ s are fitted to exponentials. In this interface, however, more relevant functions beyond Lorentzians and exponentials are implemented for analysing complex dynamics within materials. Such functions are *TeixeiraWater*, [17] diffusion in a sphere [18], rotational diffusion in a circle, [1] and Fourier transform of stretched exponentials [19]. The TeixeiraWater is implemented as a random-jump-diffusion model [17], which is more like Singwi-Sjölander jump diffusion model [20], and its application is not restricted to only water. The implemented model is defined as :

$$S(Q, \omega) = A \cdot \frac{1}{\pi} \frac{\Gamma(Q)}{\Gamma(Q)^2 + \hbar^2\omega^2} \tag{6}$$

where $\Gamma(Q)$ is the half width at half maximum (HWHM) of any Lorentzian, fitted with $S(Q, \omega)$ and A is a constant. $\Gamma(Q)$ is related with the diffusion coefficient, D, of the particle by the relation:

$$\Gamma(Q) = \frac{\hbar \cdot D \cdot Q^2}{1 + D \cdot Q^2 \cdot \tau} \tag{7}$$

where τ is a constant representing the relaxation time of the diffusion process. Similarly, diffusion-sphere model is suitable for a particle undergoing continuous diffusion confined to a spherical volume. [18] Diffusion in a rotational discrete circle is suitable for a particle undergoing discrete jumps on N-sites evenly distributed in a circle. The particle can only jump to neighbouring sites. The implemented function is the most common type of discrete rotational diffusion in a circle. [1] Fourier transform of stretched exponentials are used when a distribution of relaxation processes of several particles are involved. [19] The value of beta in the stretched exponential function determines the degree of heterogeneity among

7

particles. If beta is 1, then there is no heterogeneity and this function reduces to a single Lorentzian. Three different models are available to fit $I(Q, t)$. These are single exponential and linear combinations of two exponentials and stretched exponentials for analysing diffusive motions in different level of complexities. [1, 3]. More details of these functions may be found in Mantid webpage. [21]

To understand the nature of diffusive motions, results of fitted $S(Q, \omega)$, such as EISF (elastic incoherent structure factor) and $\Gamma(Q)$, are fitted with several models. Available models to fit $\Gamma(Q)$ are Chudley-Elliot, Hall Ross, Fickian diffusion and TeixeiraWater. Chudley-Elliot model is suitable for jump diffusion on lattice [1, 3, 23] having single jump length; Hall-Ross model is for jump diffusion in a restricted volume [3, 24] with a distribution of jump lengths, Fickian diffusion is suitable for continuous homogeneous diffusion [1, 3]; and TeixeiraWater is for random jump diffusion without confinement in a particular volume [17]. The relaxation time, τ, and jump distance, L, are used as parameters for these fits. Relevant models provided to fit EISF(Q) include diffusion confined in a spherical or cylindrical volume, and diffusion suitable for linear polycarbon chain [18, 25, 26]. In the last model the diffusion is a combination of continuous diffusion along a chain of spherical volumes of varying diameters [26]. More information about the implementation of these models is given in the next section.

3. Implementation in Mantid and Capabilities

The calculation of $S(Q, \omega)$ has been implemented in Mantid within *Indirect* → *DataReduction* interface as option $S(Q, \omega)$. A reduced file for the spectrum has to be used for this calculation. Presently data reduction option has been implemented for indirect geometry instruments. However, the data analysis interface
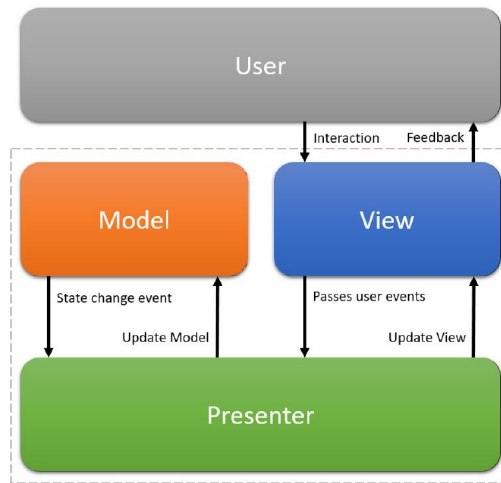
Figure 1: Model Vie Presenter (MVP) pattern is used to implement the QENS analysis interface on Mantid.

described below is independent of the geometry of instruments. The calculated $S(Q, \omega)$ is used in subsequent data analysis. Model-View-Presenter (MVP), an architectural software design pattern, is used in this implementation [22]. The MVP pattern facilitates automated unit tests as well as decoupling of the business logic, presentation logic and the graphical interface. The pattern is also useful for separating out different functionality into components which can be developed and tested simultaneously by many developers. In this pattern the 'Model' is an interface which outlines the accessible data and transformations. The 'View' defines how data is to be displayed and passes user events to the presenter. The 'Presenter' mediates between the *View* and *Model*; user events from the *View* are used to update the *Model* and data from the *Model* is formatted to be displayed in the *View*. The *View* and the *Model* never communicate with each other directly. Fig. 1 shows the MVP pattern schematically.
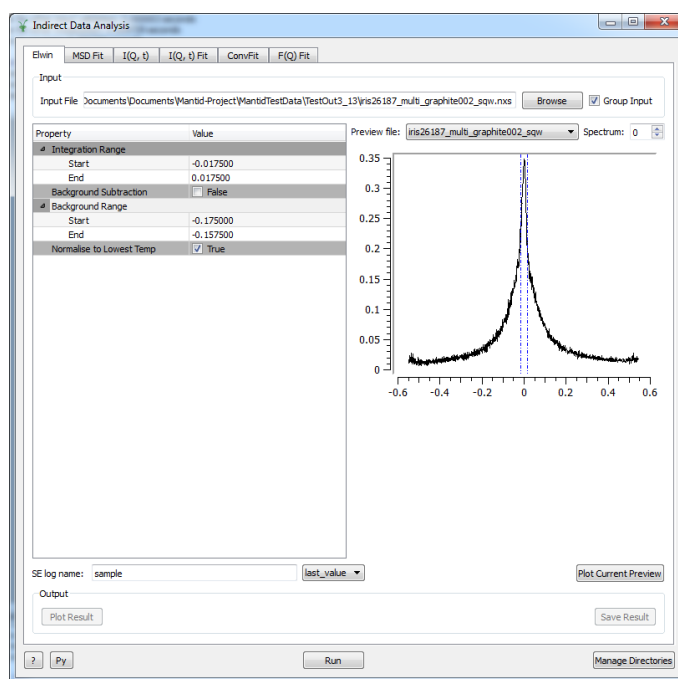
Figure 2: Elwin tab on the Data Analysis interface on Mantid.

The QENS analysis module is implemented as an interface within *Indirect* →
DataAnalysis. In this interface panel, the data analysis has been presented in five
options. The first option *Elwin* is for elastic window scan (Fig. 2), which calcu-
lates elastic intensities by integrating the elastic region of $S(Q, \omega)$. Here users can
load one or more reduced data. The corresponding temperature data are loaded
automatically from the sample log file associated with the reduced data. The range
of integration and information about the background can be supplied through the
GUI. Following the terminology of MVP pattern, the GUI of the interface panel
is implemented as *View*. The calculation of the integral has been implemented
as *Model*. *Presenter* is a set of codes which supplies information from the GUI
(*View*) to the *Model*. Thus codes represent the GUI and collect inputs never in-
teract to the *Model* directly. Implementation in this way separates the *View* from
the *Model* and any change in the configuration of GUI doesn't affect the *Model*
or vise-versa. The other advantage of this implementation is that the implemented
models can be used in python scripting without using any GUI. More discussions
about this advantage are presented at the end of this section.

Calculated $E_l(Q)$ is reported as functions of Q, Q^2, and in addition, where
the information of temperature is available, it is reported as a function of tem-
peratures. The temperature dependent $E_l(Q)$ is helpful to understand any phase
change and/or any plastic deformation due to change in temperatures. All results
or workspaces can be saved either in Nexus file format or in Ascii. The whole
workbench can also be saved as a mantid project file. The $E_l(Q)$ is then used to
calculate mean square displacements (MSD).

The *MS D* is calculated (Fig 3) by fitting to three available models, Gaussian,
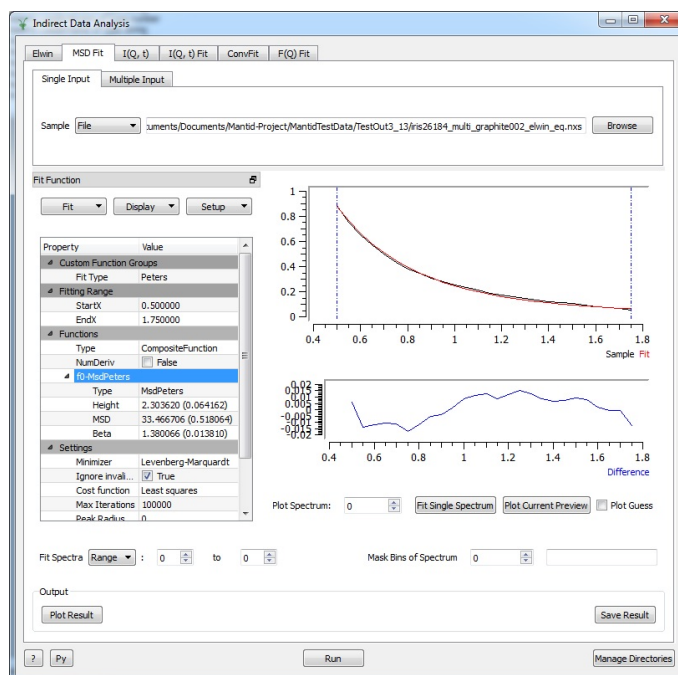Peters and Yi explained above. All fit parameters can be fixed, constrained or tied

Figure 3: MSD tab on the Data Analysis interface on Mantid showing the fitting with Peters'
model.

using options given in that interface. If a range of temperature is specified during calculations of $E_l(Q)$, the fitted MSD is reported as a function of temperatures. This MSD then can be plotted using the plotting option available at the bottom of the interface GUI, or directly from the resultant workspace file available in Mantid.

One of the main option in the *DataAnalysis* interface is the *ConvFit*. This is meant for the convolution fitting of the spectrum using the instrument resolution. A fit function can be chosen from the list of functions and the convolution of that function is calculated automatically using the user supplied resolution function of the instrument. The resolution function can be loaded either in Nexus or in Ascii format. The resultant function is then fitted with the spectrum. Only for the elastic peak, a delta function should be selected and subsequently EISF can be calculated. In the current implementation EISF is only calculated when a delta function is chosen. Options of choosing backgrounds also is provided in the interface GUI (Fig. 4). At present only sequential and individual fitting options are implemented. For individual fitting option, user can choose any particular spectrum defined by spectrum number. There is also option to select or remove particular spectrum corresponding to respective Q to avoid fitting at or near to the Bragg's peak. Several minimisers are also available including Bayesian algorithm FABADA [27, 28]. This later option provides further information, such as probability distribution functions (PDF) of cost function χ^2, which is helpful to asses the quality of the fit. The default option of the minimiser is Levenberg-Marquardt, which is a damped least square method. All other minimisers as implemented in Mantid are also available for these fittings. citefitMinimisersMantid

A number of relevant models for QENS analysis are provided in the *ConvFit*

13

to fit $S(Q, \omega)$, such as single Lorentzian, two Lorentzians, TeixeiraWater, inelastic and elastic diffusion in a sphere, inelastic and elastic rotational diffusion in discrete circles, and Fourier transform of stretched exponentials as mentioned above [1, 3, 18, 19]. These models provide options for analysing from simple homogeneous diffusion to more complex type of diffusive motions. The elastic and inelastic parts of the complex models are implemented separately to facilitate their use independently from their inelastic parts providing more freedom in analysis. The elastic parts of these models are applicable when there is any solid component (except for solid sheets), in the sample or any localised motion in the diffusion mechanism. On the other hand, inelastic parts should be used to fit the quasi-elastic part of the spectrum to analyse non-localised motions.

The plot of different workspaces, the spectrum, the fitted spectrum, the residuals, and optionally, the guess function, are made available in the right hand side of the GUI in the area of mini-plot. The axis of this mini-plot can be modified to understand the fitting better. One representative of such a plot is shown in Fig. 4. At the bottom left corner of this GUI, there is a plot option to plot HWHM ($\Gamma(Q)$) along with other parameters of the fitted spectrum as functions of Q. These plots help to understand the nature of diffusive motions within the sample.

$I(Q, t)$ is calculated by fast Fourier transformation of the reduced spectrum. A group of spectra can be transformed simultaneously. Transformation of resolution spectra are done in the same way. The latter data is used to normalise the value of $I(Q, t)$. To understand the nature of diffusive motions in the sample, calculated $I(Q, t)$ are fitted with available models, such as single exponential, linear combinations of two exponentials and stretched exponentials, for analysing diffusive motions in different level of complexities. [1, 3]. For an ideal case, one expo-
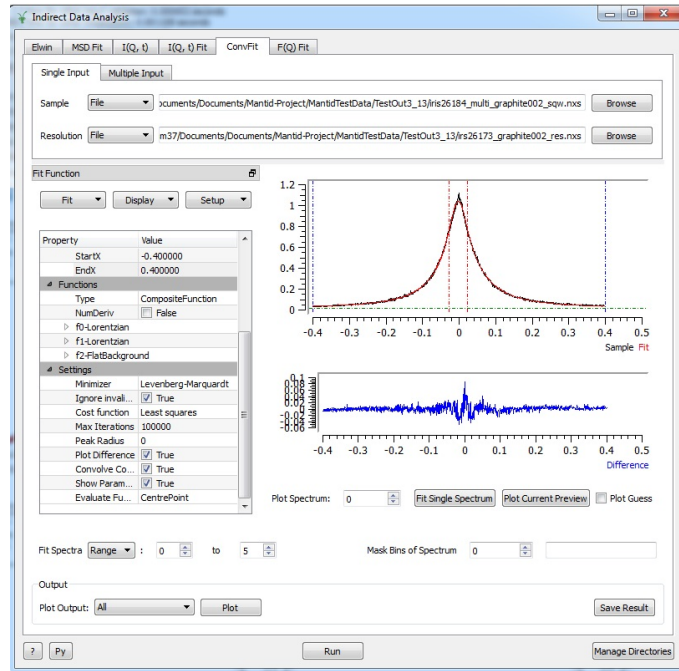
14

Figure 4: The convolution fitting interface of the QENS data anlysis on Mantid.

nential should be required to fit the $I(Q, t)$ where one Lorentzian is required to fit the corresponding $S(Q, E)$. However, due to the limited range of available E, i.e., dynamic range of any instrument, error is introduced in the calculations of $I(Q, t)$. A Monto-Carlo method is implemented to calculate this error. This error should be considered in the fitting of $I(Q, t)$ and in the calculations of diffusion coefficients. In addition to that by using tie and constrains in the fitting of $I(Q, t)$ one can achieve more global type of fit than that available to fit $S(Q, E)$. Discussions on these fit options and calculations of error will be reported elsewhere.

To analyse the nature of diffusive motions, four models, such as Chudley-Elliot, Hall Ross, Fickian diffusion and TeixeiraWater [1, 3, 23, 24] are implemented to fit calculated $\Gamma(Q)$. The relaxation time, τ, and jump distance, L, are

15

used as parameters for these fits. Three models provided to fit EISF(Q) [18, 25, 26] as explained above. The relevant parameters are radius (R) of the sphere in diffusion in sphere model [18], radius (R) and height (H) of a cylinder in the diffusion in cylinder model [25], and minimum ($R_m$in) and maximum ($R_m$ax) radius of spherical volumes in the diffusive motions in a long chain molecules [26]. These calculated parameters, such as τ, L, R etc., are reported along with the cost functions, χ^2. Calculated diffusion coefficient is also reported as a parameter.

Apart from implemented models mentioned above, users can define and use their own model within any fitting interface. To define users defined function, one has to choose *Fuctions* area on the interface browser of *FitFunctions*. The option of *user defined function* is available within the *General* section of *Fit - Select Function type* dialog. In the user defined function section, users can define the model as a function of x-axis parameter,.i.e., as a function of E or ω or Q. Currently defining functions, which are dependent on Q and E simultaneously, is not available. A model function also can be defined within a python script and the fit browser of the interface can load that model. If the model is loaded in the *ConvFit* interface, the convolution with instrument resolutions is applied automatically. More information of this facility is briefly described in Mantid documentation. [40]

Options to fit multiple datasets also have been implemented in all interfaces designed for fitting. In these options one can load more than one data set and apply models separately with individual constrains and ties. These options are helpful when different constrained are required to fit different Q ranges and/or temperatures. Within a user supplied Q range, fits are performed sequentially, however, these don't interfere other datasets where a different Q range can be loaded. Thus

an improved fitting quality can be achieved, which is almost comparable to simultaneous fitting. Dataset from different instruments also can be loaded using this facility with their different instrument resolutions. This is important for analysing data obtained from the same sample, but on different instruments.

All implemented interfaces and fitting models are available as algorithms and fit functions, respectively. It is possible to use these algorithms and functions within a python script within or outside Mantid. More advanced users, or occasional users of QENS can use this facility and tailor the script according to the requirements of their analysis. A script also can be generated from the corresponding interface GUI using the *Py* option provided. Users can deposit their own models and scripts for the use of other users in the Mantid repository of fit functions and scripts [29, 30]. More information about this scripting facility and informations about algorithms can be found elsewhere. [31, 32]

More advanced implementation of multidimentional fitting of QENS spectra using GUI is in progress. In this new GUI users will be able to load reduced files of $S(Q, \omega)$ or $I(Q, t)$ obtained from different instruments along with their instrument resolutions for a range of temperatures. Each spectra can be fitted separately in a simultaneous process and the possibility of options of tie and constrain across data and Q values will be available. This is an extension of the multiple data fitting option currently implemented. Work of the implementation of this interface is currently on-going and will be reported in future.

4. Experiments

Experiments are done on the QENS spectrometer IRIS at ISIS. [33] IRIS is a backscattering neutron instrument having energy resolution (HWHM) 17 μeV

and momentum transfer range (Q) 0.2 $Å^{-1}$ – 1.8 $Å^{-1}$. The instrument uses the 002 reflection of pyrolithic graphite analyser to achieve this high resolution. This analyser setting fixes the final energy of scattered neutron from the sample to 1.8450 meV. For testing the analysis interface, a QENS experiment is performed on a sample of water at 300 K. A 0.1 mm thin layer of water is loaded in an annular aluminium container to minimise the effect of multiple scattering. The instrument resolution is measured using a vanadium standard sample. No further correction has been applied for data analysis.

The other sample, 2,4,5 Tri Bromo Imidazole is loaded in a similar type of aluminium container having dimension of annular region of about 1 mm. The powder sample is bought from Sigma Aldrich and 1.2 g of that powder is spread homogeneously in a thin aluminium sachet before inserting that sachet into the annular container. In both cases the samples are put in a cryo-furnace at 300 K.

5. Test of the Implementation

Test of the implementation are done by analysing the QENS spectra of water by fitting the $S(Q,\omega)$ with two Lorentzians and a flat background. The interface of this fit is shown in Fig 4. A sequential fitting is done for 12 Q points as implemented in the interface. The fitted spectrum along with the experimental data are visible on the upper panel of the mini-data display window, where the lower panel shows the residue of that fitting.

The fitted spectrum for individual Q values are shown in Fig 5. The HWHM of one of these Lorentzians is independent of Q, however, the other one shows Q dependence. As shown in Fig 6, this dependency is fitted with TeixeiraWater model given in Eq.6. The best fit gives the relaxation time (τ) and diffusion coeffi-
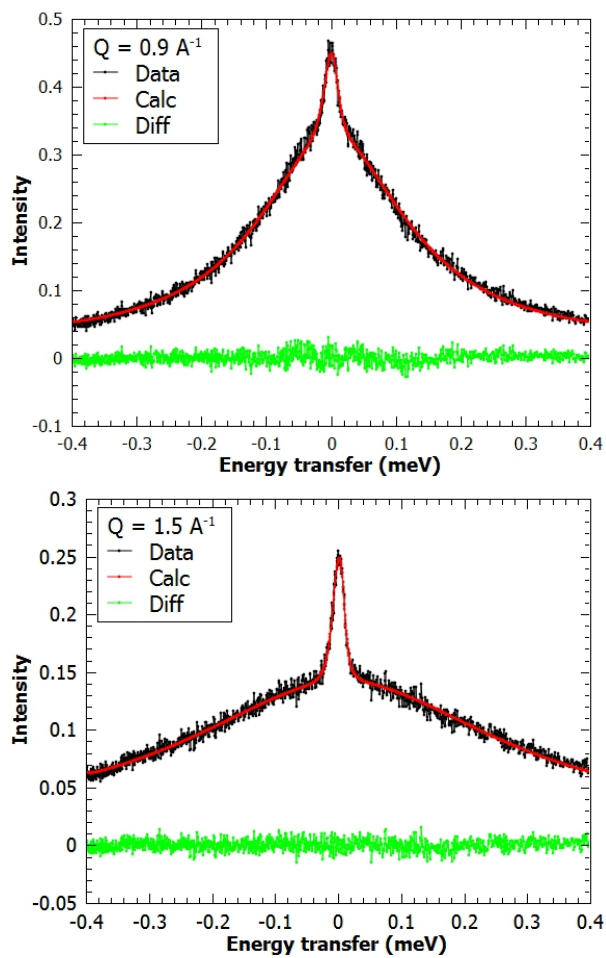
Figure 5: The convolution fitting of the QENS spectrum of water at 300 K on Mantid. The residues of the fitting are shown as Diff.
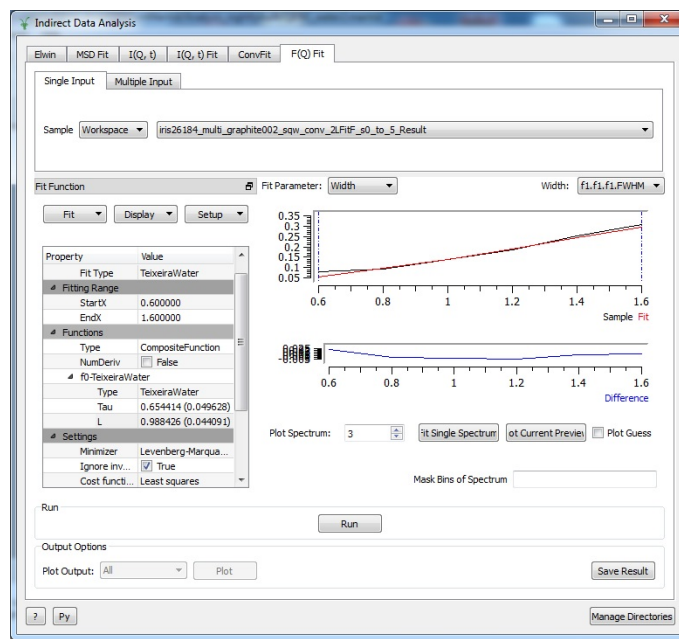
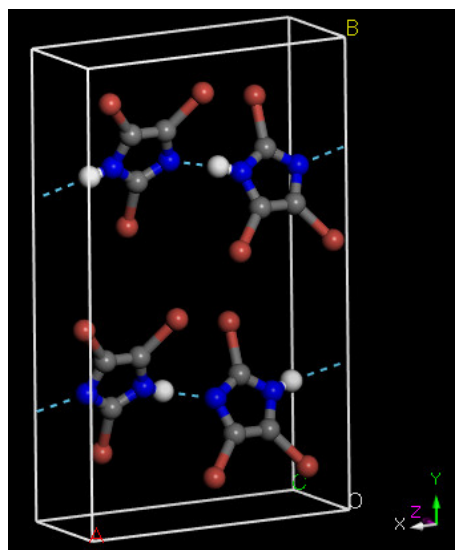Figure 6: The fitting of the FWHM(Q) of QENS spectrum on Mantid using TeixeiraWater model.

Figure 7: The crystallographic cell of $2, 4, 5Br_3$ imidazole

cient (D) as 0.65 ps and 0.25 $\text{Å}^2/ps$, respectively. The jump distance (L) reported in Fig. 6 is calculated using the relation $L^2 = 6 D\tau$. The calculated diffusion coefficient compares well with published result 0.22 $\text{Å}^2/ps$ [17, 41] validating the quality of the implementation of the interface.

6. Dynamics in 2,4,5, Tri Bromo Imidazole

With the confidence of the quality of implementation, the QENS data analysis interface is used to investigate the dynamics in organic ferroelectric material $2, 4, 5Br_3$ imidazole [34]. The dynamics of protons in such ferroelectric materials are important to understand the mechanism of ferroelectricity at room temperatures. [35–38]. The crystalographic unit cell of this material is shown in Fig. 7. The unit cell is composed of four molecular units of 2,4,5 Tribromo imidazole molecules in a orthorombic symmetry. This hydrogen bonded organic molecular

crystal shows ferroelectric polarizations at room temperature. The fitted QENS spectrum of this material is shown in Fig 8. It is found that a single Lorentzian along with a flat background and a delta function is sufficient to fit these spectra. The Q values associated with the Bragg's peak of the molecular crystal are eliminated from the fitting. The *FitS pectra* option at the bottom left corner in the interface is used for such elimination (Fig. 4).

The $\Gamma(Q)$ data obtained from the fitting with Lorentzians is fitted to various available models in the the interface to understand the dynamics of the hydrogen bonds in this material. The fitting to Hall Ross and Chudley-Elliot models with their corresponding errors are shown in Fig. 8. The value of the cost function, χ^2, for the fitting to Chudley-Elliot model is 43% higher than that for the fitting to Hall-Ross model indicating that Hall-Ross model fits better with the data. The RMS jump length and the residence time of the later model are found as 1.98 Å and 3.88 ps, respectively. The jump length and residence time of the Chudley-Elliot model are found for as 3.25 Å and 2.95 ps, respectively. The good fitting with Hall-Ross model instead of Chudley-Elliot model shows that the dynamics of proton in this material doesn't have any fixed jumping length, but a random distribution of such lengths in a restricted volume. The nature of such jumping indicates that the hydrogen bond in this material is very flexible and provide more room for proton to jump in a volume created by hydrogen bonded network of molecular units. The value of the RMS jump length is consistent with the hydrogen bond length, 2.057Å, obtained from single crystal X-ray diffraction- [34]. The jumping motion of protons across N-H–N hydrogen bond motif, similar to proton tautomerism [42], may be responsible for this diffusive motion. We are commencing temperature dependent QENS measurements and molecular dynam-

(a)

(b)

23

(c)
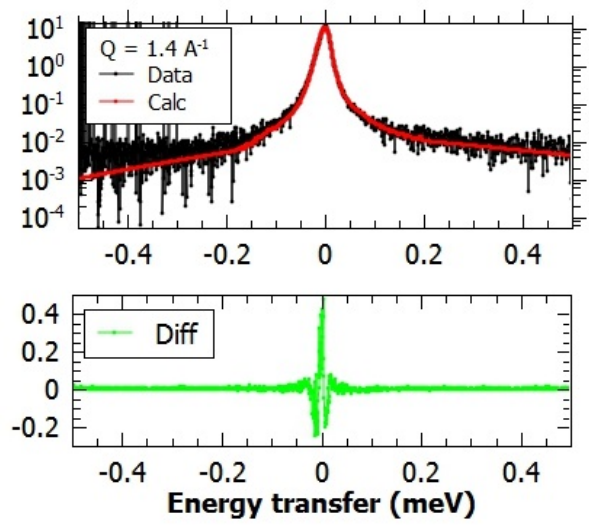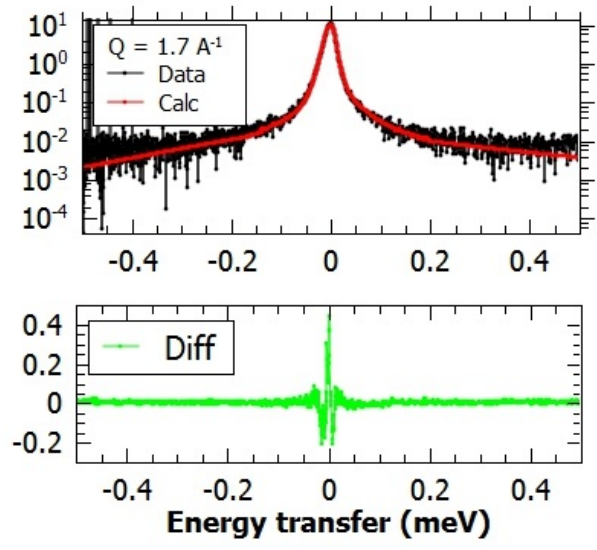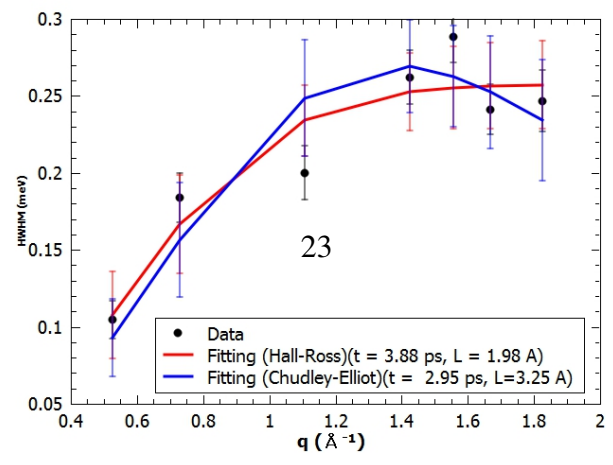
ics simulations to understand more about this jumping behaviour. More analysis on this material will be reported elsewhere.

7. Conclusions and Future Outlook

In this article we have presented the implementation of a QENS data analysis facility as an interface in the open source neutron data analysis software Mantid. The implementations are done using modern software design pattern, model-view-presenter, for easy maintenance and validations as well as efficient usability. Various options in the interface from calculations of integrals of elastic window, intermediate scattering function $I(Q, t)$ and dynamic structure factor $S(Q, \omega)$ have been implemented. Several models are also implemented in those interfaces for fitting the elastic window scan to calculate MSD to fit HWHM(Q) to understand the nature of dynamics. The implementation is validated by analysing the experiment on liquid water. The implemented interface is used to understand the proton dynamics in organic ferroelectric, 2,4,5 Tri Bromo Imidazole. Results of HWHM(Q) are fitted well to Hall-Ross model of QENS analysis. This shows that protons jumps in a confined volume in that ferroelectric. The RMS jump length obtained from the fitting is consistent with the hydrogen bond length across N-H–N motif indicating that jumping of protons across these hydrogen bonds similar to proton tautomerism may be responsible for this diffusive motion.

In future the interface will be extended to use simultaneous fitting option for fitting QENS spectra of different Q. The interface will also be extended to use of multiple data fitting on a more users friendly GUI. The work in this area is now on-going and will be reported in future.

Acknowledgements

References

[1] M. Bée, "Quasielastic Neutron Scattering", Adam Hilger, Bristol, (1988).

[2] R. Hempelmann, "Quasielastic Neutron Scattering and Solid State Diffusion", Clarendon Press, Oxford (2000).

[3] T. Springer, "Quasi-elastic neutron scattering for the diffusive motions in solids and liquids", Springer Tracts in Modern Physics **64**, 197, Springer Verlag (1972).

[4] P. S. Dubey, H. Srinivasan, V. K. Sharma, S. Mitra, V. Garcia Sakai, R. Mukhopadhyay, Sci Report., **8**, 1862 (2018).

[5] J. Armstrong, S Mukhopadhyay, F Bresme, F Fernandez-Alonso, Phys. Chem. Chem. Phys., 18, 17202 (2016).

[6] J. Wind, R. A. Mole, D. Yu, and C. D. Ling, Chem. Mater., 29, 7408 (2017).

[7] K. L. Brown, S. F Parker, I. R. García, S Mukhopadhyay, V Garcia Sakai, C Stock, Phys. Rev. B, 96, 174111 (2017).

[8] M. E Potter, A. J. O'Malley, S. Chapman, J. Kezina, S. H. Newland, I. P. Silverwood, S. Mukhopadhyay, M. Carravetta, T. M. Mezza, S. F. Parker, C. R. A. Catlow, R. Raja, ACS Catal **7**, 2926 (2017).

[9] R.T. Azuah, L.R. Kneller, Y. Qiu, P.L.W. Tregenna-Piggott, C.M. Brown, J.R.D. Copley, and R.M. Dimeo, J. Res. Natl. Inst. Stan. Technol. **114**, 341 (2009).

[10] D. Richard, M. Ferrand and G.J. Kearley, J. Neutron Res. **4**, 33, (1996).

[11] The latest version of the MANTID software package can be downloaded from dx.doi.org/10.5286/SOFTWARE/MANTID

[12] O. Arnold, et al., Nul. Instr. and Methods in Phys Res Sec A, **64**, 156 (2014).

[13] G. L. Squires, "Introduction to the theory of thermal neutron scattering", Cambridge University Press, (1978).

[14] G. Zaccai, Science **288**, 1604 (2000).

[15] J. Peters and G. R. Kneller, J. Chem. Phys **139**, 165102 (2013).

[16] Z. Yi, Y. Miao, J. Baudry, N. Jain, and J. C. Smith, J. Phys. Chem. B **116**, 5028 (2012).

[17] J. Teixeira, M. C. Bellissent-Funel, S. H. Chen, and A. J. Dianoux. Phys. Rev. A, **31**,1913 (1985).

[18] F. Volino; A. J. Dianoux, Mol. Phys., **41**, 271 (1980).

[19] F. Ganazzoli, G. Raffainia and V. Arrighib, Phys. Chem. Chem. Phys. **4**, 3734 (2002).

[20] K. S. Singwi and A. Sjolander, Phys. Rev., **119**, 863 (1960).

[21] http://docs.mantidproject.org/nightly/fitfunctions/index.html (January, 2019).

[22] M. Potel, "MVP: Model-View-Presenter the Taligent Programming Model for C++ and Java",Taligent Inc., Cuppertino, CA (1996).

[23] C. T. Chudley and R. J. Elliott, Proc. Phys. Soc. **77** 353 (1961).

[24] P. L. Hall and D. K. Ross, Mol. Phys. **36** 1549 (1978).

[25] A.J.Dianoux et al. Mol. Phys. **46** 1129 (1982).

[26] V. K.Sharma, et al., J. Phys. Chem. B **120** 154 (2016).

[27] D. Monserrat, A. Vispa, L.C. Pardo, R. Tolchenov, S. Mukhopadhyay, and F. Fernandez-Alonso, J. Phys. Conf. Ser. **663** 012009 (2015).

[28] B. L. Vidal, E. Oram, R. A. Banos, L. C. Pardo, S Mukhopadhyay, and F. Fernandez-Alonso, J. Phys. Conf. Ser. **1021** 012012 (2018).

[29] http://docs.mantidproject.org/nightly/fitting/fitfunctions/index.html#fit-functions-list (January, 2019).

[30] http://www.mantidproject.org/ScriptRepository (January, 2019).

[31] http://docs.mantidproject.org/nightly/algorithms/index.html (January, 2019).

[32] http://www.mantidproject.org/Extending_Mantid_With_Python (January, 2019).

[33] https://www.isis.stfc.ac.uk/Pages/iris.aspx

[34] M. Owczarek et al. Nature Commn. **7**, 1308 (2016).

[35] F. Fernandez-Alonso, M. J. Gutmann, S. Mukhopadhyay, D. B. Jochym, K. Refson, M. Jura, M. Krzystyniak, M. Jimenez-Ruiz, and A. Wagner: J. Phys. Soc. Japan, **82**, SA001 (2013).

[36] S. Mukhopadhyay, M. J. Gutmann, M. Jura, D. B. Jochym, M. Jimenez-Ruiz, S. Sturniolo, K. Refson, and F. Fernandez-Alonso, Chem Phys, **427**, 95 (2013).

[37] S. Mukhopadhyay, M. J. Gutmann, and F. Fernandez-Alonso, Phys Chem Chem Phys, **16**, 26234 (2014).

[38] S. Mukhopadhyay, M. J. Gutmann, M. Jimenez-Ruiz, D. B. Jochym, K. T. Wikfeldt, K. Refson and F. Fernandez-Alonso, Phys Chem Chem Phys **19**, 32216 (2017).

[39] https://docs.mantidproject.org/nightly/fitting/fitminimizers/categories/FitMinimizers.html (January, 2019).

[40] https://www.mantidproject.org/MantidPlot:_Creating_Fit_Functions (January, 2019).

[41] J. Qvist, H. Schober, and B. Halle, Chem. Phys. **134**, 144508 (2011)

[42] S. Horiuchi, K. Kobayashi, R. Kumai and S.Ishibashi, Nat. Comm. **8** 14426 (2017).